Journal of FISH BIOLOGY

fsbi An International Society for Fish Biology

Journal of Fish Biology (2014) **84**, 1300–1311
doi:10.1111/jfb.12353, available online at wileyonlinelibrary.com

Comparative squamation of the lateral line canal pores in sharks

R. W. Mckenzie*, P. J. Motta and J. R. Rohr

Department of Integrative Biology, University of South Florida, 4202 East Fowler Ave., Tampa, FL, U.S.A.

(Received 24 October 2013, Accepted 23 January 2014)

The current study collected the first quantitative data on lateral line pore squamation patterns in sharks and assessed whether divergent squamation patterns are similar to experimental models that cause reduction in boundary layer turbulence. In addition, the hypothesis that divergent orientation angles are exclusively found in fast-swimming shark species was tested. The posterior lateral line and supraorbital lateral line pore squamation of the fast-swimming pelagic shortfin mako shark *Isurus oxyrinchus* and the slow-swimming epi-benthic spiny dogfish shark *Squalus acanthias* was examined. Pore scale morphology and pore coverage were qualitatively analysed and compared. In addition, pore squamation orientation patterns were quantified for four regions along the posterior lateral line and compared for both species. *Isurus oxyrinchus* possessed consistent pore scale coverage among sampled regions and had a divergent squamation pattern with multiple scale rows directed dorsally and ventrally away from the anterior margin of the pore with an average divergent angle of 13° for the first row of scales. *Squalus acanthias* possessed variable amounts of scale coverage among the sampled regions and had a divergent squamation pattern with multiple scale rows directed ventrally away from the anterior margin of the pore with an average angle of 19° for the first row of scales. Overall, the squamation pattern measured in *I. oxyrinchus* fell within the parameters used in the fluid flow analysis, which suggests that this pattern may reduce boundary layer turbulence and affect lateral line sensitivity. The exclusively ventral oriented scale pattern seen in *S. acanthias* possessed a high degree of divergence but the pattern did not match that of the fluid flow models. Given current knowledge, it is unclear how this would affect boundary layer flow. By studying the relationship between squamation patterns and the lateral line, new insights are provided into sensory biology that warrant future investigation due to the implications for the ecology, morphology and sensory evolution of sharks.

Key words: boundary layer; divergent riblets; flow; placoid scales.

INTRODUCTION

Elasmobranchs exhibit a suite of morphological features that have contributed to their survival for > 400 million years. Two of these features, the lateral line system and placoid scales, play roles in sensory reception and protection (Reif, 1985*a*; Maruska, 2001). The lateral line system, which detects water disturbances, can be divided into two morphologically and functionally different subsystems: the canal neuromast system and the superficial neuromast system (Boord & Campbell, 1977; Peach, 2003;

*Author to whom correspondence should be addressed. Tel.: +1 772 501 0076; email: rwmckenz@mail.usf.edu

Jordan, 2008). The canal neuromast system is composed of a network of canals continuously lined by sensory neuromasts that are imbedded within the dermal collagen layer of the skin. The main canals possess periodical branching tubules that extend to the surface and either form pores that connect canal neuromasts to the outside environment or are enclosed and function as mechanotactile receptors (Jordan, 2008). Lateral line surface pores are bordered by placoid scales, which in some species are modified in size, shape and orientation (Reif, 1985*a*; Maruska, 2001).

The lateral line system of teleosts plays a functional role in rheotaxis, prey detection, predator avoidance and schooling. The morphology of the lateral line system in sharks is different from teleosts and has made behavioural role comparisons difficult (Maruska, 2001). Recent studies provide empirical evidence that the shark lateral line functions similar to that of teleosts and participates in behavioural roles such as hydrodynamic imaging, obstacle avoidance, rheotaxis, prey tracking and capture (Gardiner & Atema, 2014). In relation to this study, the pored lateral line canal neuromasts play a role in prey detection in sharks by detecting small-scale fluid accelerations, or fluid turbulences, such as those created by a prey item (Gardiner & Atema, 2007). The net turbulences in the surrounding water create pressure differences across adjacent pores, which in turn create a proportional fluid movement in the canal. This fluid movement causes cupula deflection and neuromast stimulation proportional to the fluid velocity. Therefore, the sensitivity of canal neuromasts is proportional to net outside turbulences (Coombs & Van Netten, 2005). Numerous studies of the lateral line system discuss different morphological aspects linked to the sensitivity of canal neuromasts, including canal diameter, cupula size and stiffness, innervation patterns, pore spacing and total number of pores (Johnson, 1917; Boord & Campbell, 1977; Maruska, 2001; Coombs & Van Netten, 2005; Theiss *et al.*, 2012). Few studies have examined possible sensitivity alterations caused by the placoid scales associated with lateral line pores (Tester & Kendall, 1969; Fulgosi & Gandolfi, 1983; Reif, 1985*a*).

Placoid scales, or dermal denticles, cover the shark body and display morphologies that differ dramatically among species and body regions. Placoid scales are associated with numerous functional roles including protection from predators, bioluminescence, reduction in mechanical abrasion and drag reduction (Reif, 1985*a*; Bushnell, 1991; Raschi & Tabit, 1992; Lang *et al.*, 2012). Some species of sharks, such as the shortfin mako *Isurus oxyrinchus* Rafinesque 1810, possess ribbed placoid scales that channel boundary layer flow (Bechert *et al.*, 2000) and may manipulate other boundary layer dynamics through the passive bristling of scales in certain regions of the body (Lang *et al.*, 2008, 2012; Motta *et al.*, 2012). The boundary layer is defined as the fluid layer in contact with the skin which extends outward until the tangential velocity, relative to the body, is $\leq 99\%$ of the free stream velocity (Anderson *et al.*, 2001). Species belonging to the fastest swimming sharks, including *I. oxyrinchus*, possess a highly directional patterning of scales surrounding lateral line pores (Reif & Dinkelacker, 1982). Lateral line pores of *I. oxyrinchus* possess a riblet pattern with a large number of scales adjacent to the anterior margin of the pore oriented in a divergent pattern, with scales directed both dorsally and ventrally away from the pore. Quantitative fluid flow studies conducted on riblet models with a continuous divergent riblet pattern demonstrate that a reduction of boundary layer stream-wise turbulence occurs at the point of divergence and increasing divergent riblet orientation angle reduces the amount of turbulence (Koeltzsch *et al.*, 2002; Nugroho *et al.*, 2013). It has been suggested that this reduction in boundary layer turbulence may occur at the lateral line pores of fast-swimming sharks observed with

similar squamation patterns. As canal neuromasts are sensitive to boundary layer turbulences, any change in turbulence levels would affect lateral line sensitivity. By contrast, many slow-swimming sharks, including the spiny dogfish shark *Squalus acanthias* L. 1758, possess more variable scale patterns surrounding the lateral line pores and these scales are believed to serve more for mechanical protection (Reif, 1985*a*, 1988). Therefore, it was hypothesized that the placoid scales surrounding *I. oxyrinchus* possessed pore scales with a strong divergent orientation pattern, whereas the slow-swimming *S. acanthias* would exhibit a more randomized squamation with no divergent pattern.

The purpose of this study was to address the current gap in quantitative data on lateral line pore squamation in sharks. The study addressed how lateral line pore squamation patterns change across different regions of the shark body and between two shark species possessing different lifestyles and ecology. A comparison of canal neuromast pore scale orientation patterns and divergent orientation angles was carried out, as well as a description of overall scale morphology and scale coverage of the fast-swimming pelagic *I. oxyrinchus* and the slow-swimming epi-benthic *S. acanthias*. Shark squamation patterns and divergent orientation angles were also compared to those of fluid flow models and possible functional implications were discussed. This study is the first to quantify and compare lateral line pore squamation patterns in and around sensory pores and provides new insight into functional studies of flow patterns and their effects on lateral line sensitivity in different species of sharks.

MATERIALS AND METHODS

STUDY ORGANISMS

Three fresh dead *I. oxyrinchus* [female total length (L_T) 192 cm, fork length (L_F) 171·5 cm; male L_T 158 cm, L_F 150 cm; male L_T 171·5 cm, L_F 166 cm] were obtained at the dockside from recreational fishers off the coastal waters of Montauk, New York. The specimens were wrapped in plastic at the dock and were frozen until sampling. Three preserved *S. acanthias* (male L_T 76 cm, L_F 67 cm; male L_T 71 cm, L_F 64 cm; male L_T 67 cm, L_F 59 cm) were obtained from Carolina Biological Supply (www.carolina.com/). These specimens were initially preserved in 2·5% formaldehyde solution, then washed and stored in Carosafe®, a mixture of water (89%), propylene glycol (10%) and two components ethylene glycol phenyl ether and 2-amino-2-ethyl-1,3-propanediol (1%; K. Barker, pers. comm., Carolina Biological Supply Company). Skin samples, *c*. 3 cm × 6 cm that included lateral line pores and surrounding scales were collected by scalpel from four posterior lateral line regions of the left or right flank of each shark, three of which are outlined and named by Reif (1985*a*): the mid-lateral area equidistant to the anterior- and posterior-free margin of the pectoral fin (B2), the mid-lateral area equidistant between the posterior fused margin of the first dorsal and the anterior margin of the pelvic fin (B5) and the mid-lateral region equidistant to the posterior fused margin of the pelvic fin and the anterior margin of the second dorsal fin (A2). The fourth posterior lateral line sample was taken from the mid-lateral region equidistant between the anterior and posterior fused margins of the first dorsal fin (D2). One sample of the lateral line was also taken from the supraorbital lateral line located near the mid-dorsal region equidistant between the anterior and posterior margins of the eye (SO1). Sampling was done for *I. oxyrinchus* after the specimens were thawed, during which the skin was kept moist by misting with fresh water. All research was conducted in accordance with the University of South Florida IACUC guidelines, protocol numbers T 3839 and R 3829.

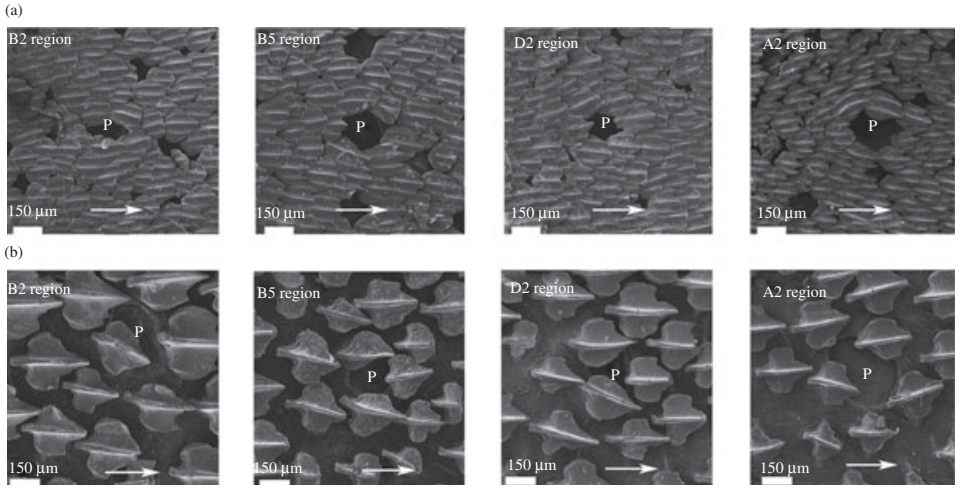

FIG. 1. Scanning electron micrographs (×100) of posterior lateral line canal neuromast pores (P) from the four sampling regions of (a) *Isurus oxyrinchus* and (b) *Squalus acanthias*. ⟹, the anterior to posterior orientation of water flow over the shark.

SAMPLING

On the intact sharks, lateral line pores were located using a stereo microscope (Meiji EMZ TR5; ×135 magnification, Meiji Techno America; www.meijitechno.com/). Posterior to the pores in each region, a transverse incision was made through the skin to expose the lateral line canal within the dermis. A 31 gauge hypodermic needle was inserted into the canal and a 50% water and India ink solution was injected to confirm the location of the canal systems tubule pores. After locating the pores, a 3 cm × 6 cm sample was removed by scalpel with the epidermis and dermis still intact from the SO1, B2, D2, B5 and A2 regions (Fig. 1). *Isurus oxyrinchus* samples were immediately frozen in fresh water. Fresh water was used for storing samples due to a lack of shark ringer solution during time of sampling. *Isurus oxyrinchus* samples were then subsequently thawed for analysis. Preserved *S. acanthias* samples were stored in Carosafe at room temperature until analysis. Placoid scales were dyed with black India ink and photographs of five lateral line pores for each of the five regions, 20 pores for each specimen, were immediately taken using a stereomicroscope (Leica M80; Leica Microsystems Inc.; www.leica-microsystems.com/) and a digital camera (3.2 MP Leica DFC295 and Leica LAS Multi-focus Software). Lateral line pores in close proximity to the edge of the sample were not used to avoid possible deformation caused by the sample removal. Excess surface moisture was removed by paper towel during exposure times and the dermis was kept moist with fresh water in between pictures to reduce shrinkage caused by desiccation. An additional 1 cm^2 piece of skin was removed from one original sample for all the body regions of both species and processed for scanning electron microscope (SEM). SEM samples were pinned down on a piece of cork board to reduce deformation and allowed to air dry for 3–4 days followed by 24 h in a 45° C vacuum oven. Traditional preservation techniques can result in shrinkage and deformation of shark skin samples. Drying the samples in this way proved to be effective in reducing curling and provided a flat surface for photography. The dried samples were placed on aluminium SEM mounts using thick carbon, double-sided adhesive tape and then also glued to the mounts with graphite conductive adhesive 154 (Electron Microscopy Sciences; www.emsdiasum.com/microscopy/default.aspx). Samples were then gold-palladium sputter-coated (Hummer Mark VI sputter coater; Anatech U.S.A.; www.anatechusa.com/). Digital SEM photographs were taken at ×30 and ×100 magnifications (TOPCON Aquila Hybrid v. 3.1.2; Topcon Positioning Systems, Inc.; www.nanounity.com/).

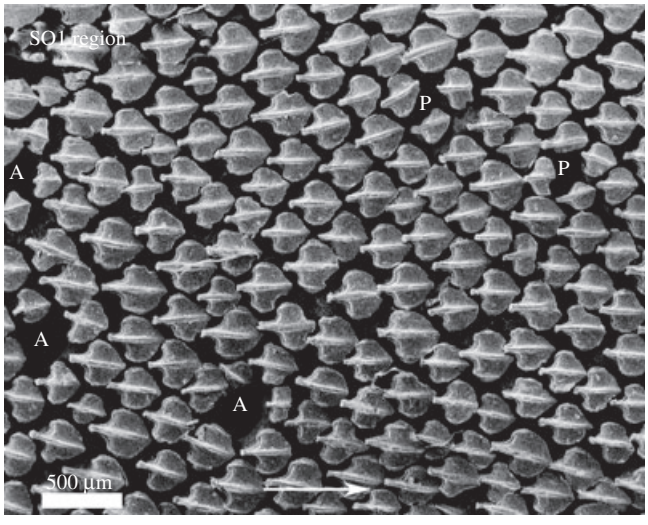

FIG. 2. Scanning electron microscope picture (×30) showing the close proximity of supraorbital canal neuromast pores (P) and adjacent ampullae of Lorenzini (A) of *Squalus acanthias*. ⟹, the anterior to posterior orientation of water flow over the shark.

Sample preserving experiments were conducted to ensure that pore scale angle measurements were accurate and did not include artefacts caused from shrinkage or swelling of the tissue during freezing or formalin fixation. The first test assessed the effects of freshwater freezing on pore scale orientation angles. Lateral line pore scale angles were measured from fresh-frozen skin samples ($n = 2$), taken from two *I. oxyrinchus* specimens, before and after being frozen in fresh water. The second test assessed the effects of fixation on pore scale orientation angles. Lateral line pore scale orientation angles were measured from skin samples ($n = 2$), taken from two fresh-frozen *I. oxyrinchus* specimens, before and after fixation following Carolina Biological Supply's protocol for *S. acanthias* specimens. Fresh-frozen specimens of *S. acanthias* were not available. All samples were analysed using scale positions V1-V5; within row one, for eight pores per treatment. The B2 and D2 regions were sampled in both cases. In total, 40 scale orientation angles covering two sharks, two regions, eight pores and five scale positions were sampled per treatment. Dried SEM-processed samples were used only for representational purposes, so they were not included in sample processing tests.

Measurements on crown width, length and morphology for both specimens were referenced from previous studies (Reif, 1985*a*). Lateral line pore pictures from each region were qualitatively examined and scale coverage was recorded. Lateral line pore pictures were also used to quantify and compare the orientation of only pore scales belonging to the posterior lateral line regions (B2, D2, B5 and A2). Supraorbital (SO1) lateral line pores were not quantified for orientation patterns because the orientation of surrounding body scales was in close proximity of neighbouring lateral line pores and pit organs that may have influenced scale orientation (Fig. 2). On each image, a digital grid was superimposed with a longitudinal axis running through the centre of the pore and approximately parallel to the longitudinal axis of the shark. Then, a vertical axis perpendicular to the longitudinal axis at the centre of the pore was constructed creating four equal-sized quadrants around each pore. The quadrants were designated Q1–Q4, starting with the anterodorsal Q1 and proceeding clockwise. Evenly spaced vertical grid lines parallel to the central vertical axis were then constructed. Lines starting from the vertical grid were drawn lengthwise over the medial riblet on each scale and scale orientation was measured by taking the angle of the medial riblet line to the vertical grid. The orientation angles of pore scales, scales within three rows extending out from the pore, were compared to the orientation angles of surrounding body scales, scales haphazardly chosen outside the three scale rows. Body scale orientation angles were measured, as described above, for five body scales per quadrant

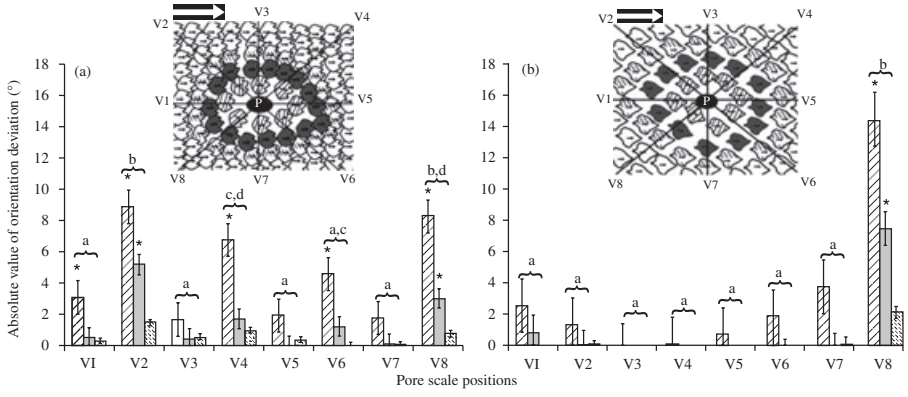

FIG. 3. Comparison of lateral line pore scale absolute orientation deviation values of (a) *Isurus oxyrinchus* and (b) *Squalus acanthias*. Pore scale orientations values were grouped by scale positions (V1–V8) and row positions (▨, row 1; ■, row 2; ▩, row 3). The baseline of 0° is equal to the average body scale orientation S.D. value of each species (*I. oxyrinchus* = 4·75°; *S. acanthias* = 5·05°), so values indicate the change in pore scale orientation above that of surrounding body scales. A schematic of lateral line pore scale picture analysis is included; scale positions (V1–V8) were sampled in a clockwise orientation 45° apart originating from the centre of the pore (P). Scales located outside of the three rows are classified as body scales (□). ⟶ on the scales indicate the approximate orientation of the riblets on the scale crown. ⟹, the approximate anterior to posterior orientation of the water flow over the shark. * above each scale position and row indicates if the absolute value of the orientation angle differs from that of the background scales for that species. The parenthesis and lower case letters above each scale position indicate if the absolute value of the orientation angle for that scale position averaged across rows differs ($P < 0{\cdot}05$) from other scale positions for that species.

surrounding the pore (Q1–Q4), for a total of 20 body scales per pore. The 20 body scale orientation angles were averaged to compute a mean ± S.D. for each pore to establish a baseline. The three rows of pore scales were then categorized. Row 1 included the scales directly abutting the pore, row 2 included the scales peripheral to row 1 scales and row 3 were those peripheral to row 2 scales. To designate which pore scales were measured for their orientation angle, a series of eight vectors were illustrated over each pore (scale positions V1–V8, Fig. 3). Each vector was placed 45° apart giving a 360° orientation analysis of the pore. The vector starting at the centre of the pore and running anteriorly along the frontal axis was labelled V1 and each subsequent vector was labelled moving in a clockwise fashion. On each of the eight vectors, the medial scale riblet angle intersecting the vectors was measured for each of the three pore scale rows. Orientation deviations were calculated by subtracting the pore scale orientation angles from the body scale baseline orientation angle. In this manner, pore scale orientation angles were compared to average body scale orientation angle within each posterior lateral line pore and among each posterior lateral line region.

STATISTICAL ANALYSIS

To test whether the preservation techniques, which differed between the two shark species, affected the scale orientation angles of *I. oxyrinchus*, a linear mixed effects model (LME) was conducted using the lme function in the nlme package of R statistical software (R core team; www.r-project.org/). The response variables were orientation angle and orientation angle deviations (deviation from background orientation angles) and the predictors were scale position around the pore, preservation technique (freezing or preserved), whether the scale orientation angle was measured before or after processing, and all possible interactions among these predictors. Scale orientation angles were nested within time of measurement (*i.e.* before or after processing), which was nested within scale position (vectors 1–5), which was nested within pore (eight pores), which was nested within sample region of the shark (two regions), which

was finally nested within shark ($n = 2$, *I. oxyrinchus*; *i.e.* position, pore, sample region and shark were treated as random effects). An interaction between preservation technique and the timing of sampling (before or after preservation) would indicate that the two preservation techniques distorted the scale angles differently.

To test for differences in pore scale orientations among sharks ($n = 3$ for *I. oxyrinchus* and *S. acanthias*), body regions (four regions), lateral line pores (64 pores), rows of scales around pores (rows 1–3) and scale positions around pores (vectors 1–8), a similar LME model was conducted within each species. These analyses also included a row-by-scale position interaction to evaluate whether the orientation angles of pore scales at the eight positions around lateral line pores depended on the distance of scale rows from these pores. Lateral line pores were nested within body regions, within sharks, and treated as random effects to ensure that proper error d.f. were achieved for each effect. If any main effects or interactions were significant, Tukey's tests were conducted in the multcomp package of R to evaluate which levels of factors or interactions were different from one another. Body scale orientations were included in these statistical analyses as a scale position and followed by Tukey's test to evaluate which scale positions around lateral line pores had orientations that differed from the orientation of these local body scales. Models were evaluated using maximum likelihood and effect significance was determined using type II likelihood ratio tests.

Raw angle data were not compared because each time the camera was moved to a new pore, the sample could have shifted altering scale orientation angles. Therefore, the deviation of pore scale orientation angles from the average angle of the background scales was used so that the analyses were relative to the background scales. The leading anterior pore scale position, V1, in *I. oxyrinchus* had scale orientations directed either dorsally or ventrally depending on the pore, which caused positive or negative orientation deviation values at different pores at the same scale position. This did not occur in *S. acanthias*, which had a consistent scale pattern among pores. In order to correct for the shift in orientation, the absolute value of pore scale orientation deviations was used to standardize the data so that all values were positive and independent of scale orientation. The absolute values of the pore scale deviations were then added to the body scale orientation baseline for each pore to compare pore scale orientations to body scale orientations.

Analysing the data in this way provided information on whether pore scales possessed a significant change in orientation pattern (orientation deviation) around the pore, which scale positions had the highest orientation deviation values, at which row the pore scales converged back to the background orientation and how these variables compared across different sharks and body regions.

RESULTS

PORE SAMPLE PROCESSING TESTS

The interaction between preservation technique (frozen *v.* formalin) and the timing of scale measurements (before and after preservation) was not significant for absolute angle (LME, d.f. = 1, $\chi^2 = 0{\cdot}391$, $P > 0{\cdot}05$) or angle deviations (relative to background scale angles; LME, d.f. = 1, $\chi^2 = 0{\cdot}122$, $P > 0{\cdot}05$). Hence, no evidence of significant angle changes was found before and after preservation or between treatments (frozen formalin).

PORE SCALE MORPHOLOGY AND SCALE COVERAGE

Lateral line pore squamation patterns varied between the two species (Fig. 1). *Isurus oxyrinchus* possessed open lateral line pores with very compact, overlapping, placoid scales with three longitudinal riblets surrounding the pores at all sampled body regions. Lateral line pores had very little scale coverage (*c.* $\leq 10\%$) on average, which varied

TABLE I. Statistical results from linear mixed effects models using the absolute value of orientation deviations that examined the effects of shark, body regions, pores, scale rows and scale positions around the lateral line pores of *Isurus oxyrinchus* and *Squalus acanthias*

		Absolute value of deviations from background scale angles of *I. oxyrinchus*		Absolute value of deviations from background scale angles of *S. acanthias*	
Effect	d.f.	χ^2	P	χ^2	P
Shark	2	6·34	<0·05	41·94	<0·001
Body region	3	4·55	>0·05	44·42	<0·001
Pore	4	2·75	>0·05	0·37	>0·05
Row	2	149·31	<0·001	100·38	<0·001
Scale position	8	126·31	<0·001	411·44	<0·001
Row × scale position	16	54·16	<0·001	55·67	<0·001

slightly between pores at all sampled body regions. *Squalus acanthias* possessed moderately covered (*c.* ≤ 50%) lateral line pores with loosely packed, non-overlapping, single-ribbed placoid scales surrounding the pores at the B2, D2, B5 and A2 regions. *Squalus acanthias* displayed compact, non-overlapping, squamation surrounding pores with very little scale (*c.* ≤10%) at the SO1 region. No significant changes in crown size have been previously observed between lateral line pore scales and body scales for either species (Reif, 1985*a*).

PORE SCALE ORIENTATION ANALYSIS

The results from the orientation analysis (Table I) indicated that *I. oxyrinchus* and *S. acanthias* had a significant change in orientation pattern from that of background body scales (scale position; LME, $\chi^2 = 126{\cdot}31$, d.f. = 8, $P < 0{\cdot}001$; LME, $\chi^2 = 411{\cdot}44$, d.f. = 8, $P < 0{\cdot}001$). Significant differences in the orientation deviation values were seen between pore scale positions averaged across scale rows for *I. oxyrinchus* [row: LME, $\chi^2 = 149{\cdot}31$, d.f. = 2, $P < 0{\cdot}001$, Fig. 3(a)] and *S. acanthias* [row: LME, $\chi^2 = 100{\cdot}38$, d.f. = 2, $P < 0{\cdot}001$, Fig. 3(b)]. There were no significant differences in pore scale orientation deviation values among the four posterior lateral line regions for *I. oxyrinchus* (body region: LME, $\chi^2 = 4{\cdot}55$, d.f. = 3, $P > 0{\cdot}05$). There were significant differences in pore scale orientation deviations among the four posterior lateral line regions for *S. acanthias* (body region: LME, $\chi^2 = 44{\cdot}42$, d.f. = 3, $P < 0{\cdot}001$). Tukey's test indicated that the B2 region was significantly different from the D2 ($P < 0{\cdot}05$), B5 ($P < 0{\cdot}001$) and A2 ($P < 0{\cdot}001$) regions. The D2 region was also significantly different from the B5 region ($P < 0{\cdot}05$).

Tukey's tests indicated that *I. oxyrinchus* had significant orientation deviations in row 1 at scale positions V1, V2, V4, V6 and V8 [$P < 0{\cdot}05$, Fig. 3(a)]. Significant orientation deviations from background scales were still observed at scale positions V2 and V8 in row 2. No significant orientation deviations were observed in row 3, the outermost pore scale row measured, for any pore scale positions. For *S. acanthias*, Tukey's tests indicated that significant orientation deviations occurred in row 1 and row 2 at scale position V8 with the scales angled ventrally [$P < 0{\cdot}05$, Fig. 3(b)]. No significant

orientation deviations were observed at scale position V8 in row 3. Scale positions V1–V7 did not show significant orientation deviations in any rows. Therefore, for both species, the significant changes in scale orientation patterns end after two rows of scales moving away from the pore. When absolute orientation deviations averaged across rows for each scale position within each species were compared, *I. oxyrinchus* had numerous differences whereas *S. acanthias* only differed at one scale position. In *I. oxyrinchus* scale positions, V1, V3, V5, V6 and V7 did not differ among each other but differed from all other scale positions [Fig. 3(a)], except for V6 which formed a group with scale position V4. Scale positions V2 and V8 did not differ from each other and formed a group. Scale positions V4 and V8 also did not differ from each other and formed a separate group. In *S. acanthias*, only scale position V8 differed from all other scale positions [Fig. 3(b)].

Two different scale patterns occurred for each species [Fig. 3(a), (b)]. For *I. oxyrinchus*, the pattern was: vector 1, extending anterior along the mid-lateral plane of the pore, possessed varying divergent scale orientation patterns directed either dorsally or ventrally away from the pore. Vector 2, extending anteriodorsally from the pore, possessed divergent scale orientations directed dorsally away from the pore. Vector 8, extending anterioventrally from the pore, possessed divergent scale orientations directed ventrally away from the pore. There were no modifications in scale orientations of vectors 3 and 7. Vector 4, extending posteriodorsally from the pore, possessed convergent scale orientations directed ventrally to the pore. Vector 6, extending posterioventrally from the pore, possessed convergent scale orientations directed dorsally to the pore. There were no orientation modifications of vector 5, extending posteriorly from the pore. Therefore, scales possessed a divergent pattern around the pore at the anterior margin of the pore and a convergent pattern to the pore at the posterior margin in *I. oxyrinchus*. *Squalus acanthias* possessed a divergent scale pattern exclusively at the anterioventral margin of the pore.

DISCUSSION

PORE SCALE MORPHOLOGY AND SCALE COVERAGE

Scale crown morphology and size often change among different regions and features of the shark body; however, no significant differences occurred between lateral line pore scales and surrounding body scales in either *I. oxyrinchus* or *S. acanthias* (Reif, 1985*a*). Both *I. oxyrinchus* and *S. acanthias* displayed differing amounts of lateral line pore scale coverage. *Isurus oxyrinchus* possessed open pores with little scale coverage surrounded by tightly grouped scales throughout the supraorbital and posterior lateral line canals. Open lateral line pores with little scale coverage have also been previously observed in other species including the blue shark *Prionace glauca* (L. 1758) and little sleeper shark *Somniosus rostratus* (Risso 1827), both of which have divergent scale orientations around the pores (Fulgosi & Gandolfi, 1983; Reif, 1985*b*). *Squalus acanthias* possessed open pores with little scale coverage surrounded by loosely packed scales at the supraorbital lateral line canal. Pores along the posterior lateral line canal, which extended down the flank of the shark, were moderately covered. Similar regional changes in lateral line pore coverage are also present in some *Carcharhinus* species, which have open lateral line pores at the cephalic canals but have completely covered

pores along the posterior lateral line with modified notched scales (Tester & Kendall, 1969). Variable amounts of scale coverage are also seen in the superficial neuromast systems of sharks, also known as pit organs. Some species including *I. oxyrinchus* have completely covered pit organs, whereas species such as the Port Jackson shark *Heterodontus portjacksoni* (Meyer 1793) have superficial neuromasts in loosely covered pits. The underlying factors influencing lateral line scale coverage in elasmobranchs are still unknown (Peach & Rouse, 2004).

PORE SCALE ORIENTATION PATTERNS

On the lateral flank of the shark body, scale riblets are generally oriented in a consistent anterior to posterior direction (Reif, 1985*a*). Highly directional orientation patterns have been observed in the vicinity of lateral line pores in some fast-swimming species of sharks (Reif & Dinkelacker, 1982; Reif, 1985*a*). Orientation patterns surrounding the lateral line pores have never been quantified or compared between species until now. Two significant and unique divergent orientation patterns were measured in *I. oxyrinchus* and *S. acanthias* (Fig. 1). *Isurus oxyrinchus* possessed a multi-rowed divergent pattern anterior to the pore with scales oriented dorsally and ventrally from the pore. By contrast, pore scales at the posterior margin of the pore within the first row were oriented in a convergent pattern with scales oriented ventrally and dorsally to the pore. *Squalus acanthias* possessed a multi-rowed divergent pattern anterioventrally to the pore with scales exclusively oriented ventrally away from the pore. Divergent riblet models, comparable to *I. oxyrinchus*, resulted in a reduction (*c.* 8 to 22%) of boundary layer turbulence at different levels depending on the degree (10 to 30°) of divergent riblet angle (Koeltzsch *et al.*, 2002; Nugroho *et al.*, 2013). The average divergent orientation angles in the first row of *S. acanthias* (*c.*19°) and *I. oxyrinchus* (*c.*13°) fell within the range tested in the fluid flow models. Therefore, based on the models, both study specimens possessed divergent orientation angles high enough to create significant reductions in boundary layer turbulence.

Lateral line canal neuromasts are sensitive to small-scale fluid flow turbulences in the near field environment (Coombs & Van Netten, 2005). Small-scale turbulences, or accelerations, in the surrounding water create pressure differences across adjacent pores, creating fluid movement in the canal, which causes cupula deflection and neuromast stimulation proportional to net turbulences. The reduction of environmental turbulences could, therefore, alter lateral line sensitivity. Reduction of the boundary layer turbulent intensity at lateral line canal pores would proportionally decrease the fluid velocity within the canal. Reductions of canal fluid velocity are induced by other morphological features in fishes, such as the narrowing of canals before the canal neuromast (Coombs & Van Netten, 2005). Narrowing of the canals reduces responsiveness of the canal neuromasts at low frequencies and increases the cut-off frequency to which canal neuromasts can function. The increase in high-frequency sensitivity may be useful for species in highly turbulent environments. Functional considerations based on current models must be considered with caution because the fluid flow models do not take into account the fluid dynamics of the open pore. In addition, *S. acanthias* possessed an exclusively ventral oriented divergent scale pattern that does not match the herring bone dorsal and ventral divergent orientation pattern found in both *I. oxyrinchus* and fluid flow models. Therefore, more fluid flow analysis is needed to fully understand the implications of pore squamation on lateral line sensitivity.

If lateral line sensitivity is linked to surrounding scale orientation patterns and the degree of divergent angle, then regional differences in the orientation patterns along the shark body could have ecological and functional implications. Lateral line pore scale orientation angles and patterns were homologous among the four posterior lateral line regions of *I. oxyrinchus*. By contrast, *S. acanthias* possessed slight changes in the pore scale orientation angles between the B5, D2 and B2 regions of the body. B2, located just posterior of the gills, possessed significantly higher divergent pore scale angles when compared to other body regions of *S. acanthias*. The higher divergent pore scale angle might indicate enhanced turbulence reduction in this region due to an in increase in boundary layer turbulence caused by water exiting the gills. The findings, however, were confounded by *I. oxyrinchus*, which had no changes in divergent pore scale angle at the B2 region.

In summary, this study was the first to quantify and compare lateral line canal neuromast pore squamation orientations in sharks. Divergent scale orientations, scale coverage and scale morphology varied between different body regions and between the two study species. Two different divergent orientation patterns surrounding the lateral line pores were present between the species, which confounds previous hypotheses linking divergent squamation patterns exclusively to fast-swimming species. The divergent orientation pattern and angles seen in *I. oxyrinchus* were similar to that of fluid flow models, which decrease boundary layer turbulence. Altering the boundary layer turbulence level affects the sensitivity of the lateral line, which plays vital behavioural roles in hydrodynamic imaging, obstacle avoidance, rheotaxis, prey tracking and capture (Gardiner & Atema, 2014). *Squalus acanthias* possessed slightly higher divergent angles than *I. oxyrinchus* arranged in an exclusively ventral oriented divergent pattern. The orientation pattern of *S. acanthias* has yet to be modelled and possible boundary layer effects are unknown at this time. The relationship between lateral line pores and placoid scales described in this study provides a new insight and warrants future investigation due to its implications for the ecology, morphology and sensory evolution of sharks.

The authors thank P. Majeski and J. Majeski and crew and M. Sampson, A. VanWormer, K. Deiter, P. Pegley, B. Augsburger, J. Morris and the Mote Marine Laboratory for providing shark specimens. They also thank C. Steffan and E. Haller for their assistance with the scanning electron microscopy. They also convey special thanks to the reviewers for their suggestions and improvements on this manuscript. This research was supported by a Collaborative National Science Foundation grant CBET 0932026 to P.J.M., the Porter family Foundation and the Department of Integrative Biology, University of South Florida.

References

Anderson, E. J., McGillis, W. R. & Grosenbaugh, M. A. (2001). The boundary layer of swimming fish. *Journal of Experimental Biology* **204,** 81–102.

Bechert, D. W., Bruse, M. & Hage, W. (2000). Experiments with three-dimensional riblets as an idealized model of shark skin. *Experiments in Fluids* **28,** 403–412. doi: 10.1007/s003480050400

Boord, R. L. & Campbell, C. B. G. (1977). Structural and functional organization of the lateral line system of sharks. *American Zoologist* **17,** 431–441.

Bushnell, D. M. (1991). Drag reduction in nature. *Annual Review of Fluid Mechanics* **23,** 65–79. doi: 10.1146/annurev.fl.23.010191.000433

Coombs, S. & Van Netten, S. M. (2005). The hydrodynamics and structural mechanics of the lateral line system. *Fish Physiology* **23,** 103–139. doi: 10.1016/S1546-5098

Fulgosi, F. C. & Gandolfi, G. (1983). Re-description of the external morphology of *Somniosus rostratus* (Risso, 1826), with special reference to its squamation and cutaneous sensory organs, and aspects of their functional morphology (Pisces Selachii Squalidae). *Monitore Zoologica Italiano (N.S.)* **17,** 27–70.

Gardiner, J. M. & Atema, J. (2007). Sharks need the lateral line to locate odor sources: rheotaxis and eddy chemotaxis. *Journal of Experimental Biology* **210,** 1925–1934. doi: 10.1242/jeb.000075

Gardiner, J. M. & Atema, J. (2014). Flow sensing in sharks: lateral line contributions to navigation and prey capture. In *Flow Sensing in Air and Water: Behavioral, Neural, and Engineering Principles of Operation* (Bleckmann, H., Mogdans, J. & Coombs, S. L., eds), pp. 127–146. Berlin: Springer-Verlag.

Johnson, S. E. (1917). Structure and development of the sense organs of the lateral canal system of selachians (*Mustelus canis* and *Squalus acanthias*). *Journal of Comparative Neurology* **28,** 1–74. doi: 10.1002/cne.900280102

Jordan, L. K. (2008). Comparative morphology of stingray lateral line canal and electrosensory systems. *Journal of Morphology* **269,** 1325–1339. doi: 10.1002/jmor.10660

Koeltzsch, K., Dinkelacker, A. & Grundmann, R. (2002). Flow over convergent and divergent wall riblets. *Experiments in Fluids* **33,** 346–350. doi: 10.1007/s00348-002-0446-3

Lang, A. W., Hidalgo, P., Motta, P. J. & Westcott, M. (2008). Bristled shark skin: a microgeometry for boundary layer control? *Bioinspiration & Biomimetics* **3,** 1–9. doi: 10.1088/1748-3182/3/4/046005

Lang, A., Habegger, M. & Motta, P. (2012). Shark skin drag reduction. In *Encyclopedia of Nanotechnology*, Vol. 19 (Bhushan, B., ed), pp. 2394–2400. Berlin: Springer. doi: 10.1007/978-90-481-9751-4_266

Maruska, K. P. (2001). Morphology of the mechanosensory lateral line system in elasmobranch fishes: ecological and behavioral considerations. *Environmental Biology of Fishes* **60,** 47–75. doi: 10.1023/A:1007647924559

Motta, P., Habegger, M. L., Lang, A., Hueter, R. & Davis, J. (2012). Scale morphology and flexibility in the shortfin mako *Isurus oxyrinchus* and the blacktip shark *Carcharhinus limbatus*. *Journal of Morphology* **273,** 1096–1110. doi: 10.1002/jmor.20047

Nugroho, B., Hutchins, N. & Monty, J. P. (2013). Large-scale spanwise periodicity in a turbulent boundary layer induced by highly ordered and directional surface roughness. *International Journal of Heat and Fluid Flow* **41,** 90–102. doi: 10.1016/j.ijheatfluidflow.2013.04.003

Peach, M. B. (2003). The behavioral role of pit organs in the epaulette shark. *Journal of Fish Biology* **62,** 793–802. doi: 10.1046/j.1095-8649.2003.00065.x

Peach, M. B. & Rouse, G. W. (2004). Phylogenetic trends in the abundance and distribution of pit organs of elasmobranchs. *Acta Zoologica* **85,** 233–244. doi: 10.1111/j.0001-7272.2004.00176.x

Raschi, W. & Tabit, C. (1992). Functional aspects of placoid scales: a review and update. *Marine & Freshwater Research* **43,** 123–147. doi: 10.1071/MF9920123

Reif, W. E. (1985*a*). Squamation and ecology of sharks. *Courier Forschungsinstitut Senckenberg* **78,** 1–255.

Reif, W. E. (1985*b*). Morphology and hydrodynamic effects of the scales of fast swimming sharks. *Fortschritte der Zoologie* **30,** 483–485.

Reif, W. E. (1988). Evolution of high swimming velocities in sharks – a case of escalation? *Neues Jahrbuch für Geologie und Palaeontologie, Abhandlungen* **194,** 361–379.

Reif, W. E. & Dinkelacker, A. (1982). Hydrodynamics of the squamation in fast swimming sharks. *Neues Jahrbuch für Geologie und Palaeontologie, Abhandlungen* **164,** 184–187.

Tester, A. L. & Kendall, J. I. (1969). Morphology of the lateralis canal system in the shark genus *Carcharhinus*. *Pacific Science* **23**, 1–16. http://hdl.handle.net/10125/3362

Theiss, S. M., Collin, S. P. & Hart, N. S. (2012). The mechanosensory lateral line system in two species of wobbegong shark (Orectolobidae). *Zoomorphology* **131,** 339–348. doi: 10.1007/s00435-012-0161-4